Linear Viscoelastic Behavior of Some Incompatible Polymer Blends in the Melt. Interpretation of Data with a Model of Emulsion of Viscoelastic Liquids

3 **AUTHORS**, INCLUDING:

Didier Greabling
Université de Pau et des Pays de l'Adour
17 PUBLICATIONS **593** CITATIONS

SEE PROFILE

Linear Viscoelastic Behavior of Some Incompatible Polymer Blends in the Melt. Interpretation of Data with a Model of Emulsion of Viscoelastic Liquids

D. Graebling,* R. Muller, and J. F. Palierne

Institut Charles Sadron (EAHP-CRM), 4 rue Boussingault, 67000 Strasbourg, France

ABSTRACT: The linear viscoelastic behavior of two-phase polymer blends in the melt has been analyzed by an emulsion model, with takes into account the viscoelasticity of the phases. In this paper, we have studied two types of blends: PS/PMMA and PDMS/POE-DO. For PS/PMMA blends, the model leads to values of relaxation times and secondary plateau modulus in accordance with experimental data. This supports the assumption that long-time relaxation mechanisms are due to geometrical relaxation of the droplets of the dispersed phase. For a quantitative comparison, further experiments have been carried out on PDMS/POE-DO blends for which the distribution of size of the dispersed POE-DO inclusions may be easily determined. The data confirm the validity of the model and show that dynamic shear measurements can be used as a method to determine the interfacial tension between two polymer melts.

I. Introduction

The rheological behavior of multiphase polymer melts has become a subject of great interest owing to the increasing use of polymer blends. If the melt rheology of incompatible polymer blends is compared to that of individual phases, it is quite generally observed that multiphase polymer melts show pronounced elastic properties and very long relaxation time processes. This is well illustrated in Figure 1, showing the curves of dynamic moduli versus frequency for a two-phase polymer blend compared to the same curves for the phases. The values of the storage modulus at low frequencies for the blend are more than one decade above those for the phases. It is the purpose of the present paper to show that for polymer blends forming a dispersion, the deformability of droplets of the minor phase during the macroscopic deformation can give rise to mechanical relaxation times of the same order of magnitude as the long relaxation times observed experimentally. With this aim in view, it will be shown that quantitative agreement between predictions of emulsion-type models and linear viscoelastic data on selected polymer blends can be found.

The rheology of heterophase media has been extensively studied from a theoretical point of view for several decades.[1-12] Palierne recently considered the linear viscoelastic behavior of concentrated emulsions of incompressible viscoelastic materials in the presence of an interfacial agent.[13] He worked out a linear viscoelastic constitutive equation for the emulsion as a function of the linear viscoelastic behavior of the phases, the size distribution of the dispersed droplets, and the interfacial tension.

This result is of particular interest for heterogeneous polymer blends in the melt, and it will be used as the theoretical framework to analyze rheological tests on PS/PMMA and PDMS/POE-DO blends. All data of the present study have been obtained in the oscillatory shear mode at small strain amplitudes, which allows direct comparison with the theoretical expression of the complex modulus $G^* = G' + iG''$, and prevent the morphology from being affected by the rheological experiment (like, for instance, droplet breakup in steady shear or extensional flow).[3,4,14]
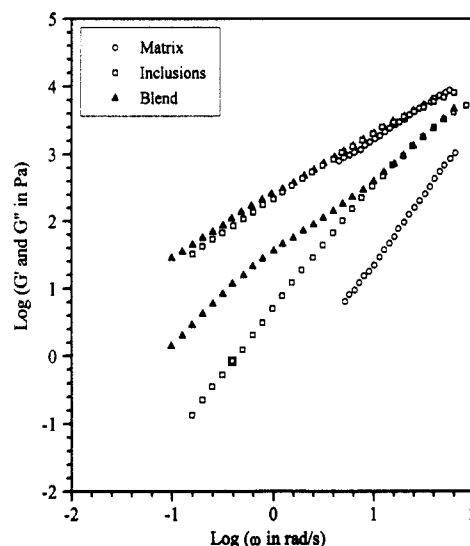

Figure 1. Dynamic moduli vs frequency. Comparison between two-phase polymer blend and the phases.

II. Theoretical Expression of G^* for a Blend

The systems that are considered in ref 13 and to which belong the polymer blends investigated here are emulsions of viscoelastic incompressible materials, where the droplets forming the dispersed phase are spherical in equilibrium. A distribution of size and composition of the dispersed phase can be taken into account, as well as the dependence of interfacial tension on local shear deformation and variation of area during deformation of dispersed droplets.

The main assumption leading to the constitutive equation of the emulsion is that the droplet deformation remains small. This means that the theory only predicts linear viscoelastic behavior so that comparison with experimental data is only valid if the latter have actually been obtained in the linear range (i.e., small strain amplitudes for oscillatory measurements).

If the interfacial tension between the matrix and the dispersed phase is assumed to be independent of local shear and variation of interfacial area, the following simplified expression for the complex shear modulus of the emulsion is obtained:

$$G^*(\omega) = G^*_m(\omega)\frac{1 + 3\sum_i \phi_i H_i(\omega)}{1 - 2\sum_i \phi_i H_i(\omega)}$$

$$H_i(\omega) = \{4(\alpha/R_i)[2G^*_m(\omega) + 5G^*_i(\omega)] +$$
$$[G^*_i(\omega) - G^*_m(\omega)][16G^*_m(\omega) + 19G^*_i(\omega)]\}/$$
$$\{40(\alpha/R_i)[G^*_m(\omega) + G^*_i(\omega)] +$$
$$[2G^*_i(\omega) + 3G^*_m(\omega)][16G^*_m(\omega) + 19G^*_i(\omega)]\} \quad (1)$$

where $G^*_i(\omega)$, $G^*_m(\omega)$, and $G^*(\omega)$ are respectively the complex moduli of the dispersed phase, matrix, and emulsion at frequency ω, α is the interfacial tension, and ϕ_i is the volume fraction of inclusions of radius R_i. It appears that comparison of eq 1 to experimental G^* data on two-phase blends is straightforward, if data for the dynamic moduli of the pure phases are available in the same frequency range and if the morphology (ϕ_i, R_i) and interfacial tension are known. Equation 1 can also be used together with viscoelastic measurements to estimate the interfacial tension as the value of α leading to the best fit between the above expression and experimental data. The precision of this estimation is then directly related to that on the morphology, since one determines in fact the ratio α/R.

It is interesting to note that eq 1 includes several results of the literature as special cases. For rigid spheres dispersed in a viscoelastic matrix ($G^*_i(\omega) \rightarrow \infty$), $H_i(\omega) = 0.5$ and

$$G^*(\omega) = G^*_m(\omega)\left(\frac{1 + {}^3/_2\phi}{1 - \phi}\right) \quad (2)$$

If the matrix is a Newtonian liquid ($G^*_m(\omega) = i\omega\eta_m$), eq 2 amounts to Einstein's result.[1,2] For a dispersion of viscoelastic materials without interfacial tension ($\alpha = 0$)

$$G^*(\omega) = G^*_m(\omega) \times$$
$$\left(\frac{2G^*_i(\omega) + 3G^*_m(\omega) + 3\phi[G^*_i(\omega) - G^*_m(\omega)]}{2G^*_i(\omega) + 3G^*_m(\omega) - 2\phi[G^*_i(\omega) - G^*_m(\omega)]}\right) \quad (3)$$

which legitimates Dickie's result.[11] If the phases are elastic solids ($G^*_i(\omega) = G_i$, $G^*_m(\omega) = G_m$), Kerner's expression[8] for incompressible materials ($\nu = 0.5$) is obtained.

Since we focus here on polymer blends in the melt, we now examine the ability of the model to predict experimental phenomena in emulsions of viscoelastic liquids like, for instance, the data in Figure 1. For the sake of simplicity, we first write out the expression of the complex modulus of an emulsion of two Newtonian liquids with uniform size ($R_i = R$) of dispersed droplets and constant interfacial tension. If η_i and η_m are the viscosities of the dispersed phase and matrix, then $G^*_i(\omega) = i\omega\eta_i$, and $G^*_m(\omega) = i\omega\eta_m$, and eq 1 amounts to

$$G^*(\omega) = i\omega\eta_0\frac{1 + i\omega\lambda_2}{1 + i\omega\lambda_1} \quad (4)$$

where

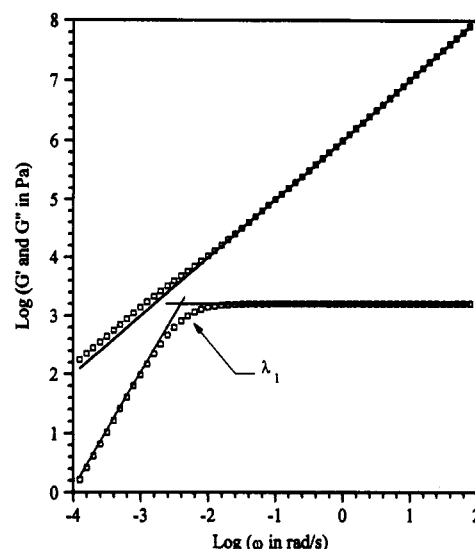$$\eta_0 = \eta_m\frac{10(K + 1) + 3\phi(5K + 2)}{10(K + 1) - 2\phi(5K + 2)} \quad (5)$$

Figure 2. Dynamic moduli vs frequency; theoretical behavior for a blend of two Newtonian liquids.

$$\lambda_1 = \frac{R\eta_m}{4\alpha}\frac{(19K + 16)(2K + 3 - 2\phi(K - 1))}{10(K + 1) - 2\phi(5K + 2)} \quad (6)$$

$$\lambda_2 = \frac{R\eta_m}{4\alpha}\frac{(19K + 16)(2K + 3 + 3\phi(K - 1))}{10(K + 1) + 3\phi(5K + 2)} \quad (7)$$

η_0 is the zero-shear viscosity of the emulsion, which is found to be always above that of the matrix liquid, λ_1 a relaxation time, and λ_2 a retardation time; $K = \eta_i/\eta_m$ is the viscosity ratio.

The spring-and-dashpot analog for eq 4 is a Jeffreys model consisting of a Maxwell element (G_1, η_1) in parallel with a dashpot η_2. The following relations hold between G_1,η_1,η_2 and $\eta_0,\lambda_1,\lambda_2$:

$$\eta_0 = \eta_1 + \eta_2 \qquad \lambda_1 = \eta_1/G_1 \qquad \lambda_2 = \frac{\eta_1\eta_2}{(\eta_1 + \eta_2)G_1} \quad (8)$$

It appears that the model predicts viscoelastic behavior for an emulsion of purely viscous liquids. Figure 2 shows the calculated $G'(\omega)$ and $G''(\omega)$ curves for $\eta_m = \eta_i = 10^6$ Pa·s, $R = 1$ μm, $\alpha = 10$ mN/m, and $\phi = 0.2$. The high-frequency plateau observed for G' is equal to G_1 and can be written as a function of the emulsion parameters:

$$G_1 = 20\frac{\alpha}{R}\phi\frac{1}{(2K + 3 - 2\phi(K - 1))^2} \quad (9)$$

Relaxation time λ_1 corresponds to the time required for a deformed droplet to recover its spherical equilibrium shape. With typical values of emulsion parameters for blends of molten polymers, this time can be of the order of seconds to minutes. The above expressions for λ_1 and G_1 show that the interfacial tension between two Newtonian liquids can in principle be determined from dynamic mechanical measurements provided the viscosities, volume fraction, and droplet radius of the dispersed phase are known.

Since polymer melts are viscoelastic liquids, the above Newtonian analysis is only valid at very low frequencies where $G'_m \ll G''_m$ and $G'_i \ll G''_i$. To account for the frequency dependence of a polymer blend over the whole frequency range, we have to consider the blending law in the case of viscoelastic phases. It will be possible to define characteristic relaxation times and moduli for such a system in the most simple case where all dispersed droplets have the same radius R and where both phases are described by single relaxation time Maxwell models:

$$G^*_m(\omega) = \frac{i\omega\eta_m}{1 + i\omega\lambda_m}$$

$$G^*_i(\omega) = \frac{i\omega\eta_i}{1 + i\omega\lambda_i} \qquad (10)$$

η_m, λ_m, $G_m = \eta_m/\lambda_m$, η_i, λ_i, and $G_i = \eta_i/\lambda_i$ are the viscosities, relaxation times, and moduli for the matrix and dispersed phase, respectively. The ratios of viscosities $K = \eta_i/\eta_m$, moduli $k = G_i/G_m$, and relaxation times $\chi = \lambda_i/\lambda_m$ satisfy the relation $K = k\chi$.

A typical G' vs frequency curve calculated from eq 1 and using expression 10 of the complex moduli of the phases is shown in Figure 3. The emulsion parameters R, ϕ, α, η_i, and η_m are the same as in Figure 2 and $\lambda_i = \lambda_m = 0.1$ s. Four frequency zones and three characteristic relaxation times can be distinguished on the curves in Figure 3: a plateau zone for G' ($G' = G$) at frequencies higher than $1/\lambda_M$. In the range $[1/\lambda_P, 1/\lambda_M]$, the frequency dependence of the moduli is very close to $G' \propto \omega^2$, $G'' \propto \omega$. A secondary plateau in G' ($G' = G_P$) appears for frequencies in the range $[1/\lambda_D, 1/\lambda_P]$. Finally, at frequencies lower than $1/\lambda_D$, the terminal zone of the emulsion is reached.

λ_M can be thought of as some mean relaxation time of the phases; it will in general be of the order of λ_m, the relaxation time of the matrix. λ_D is the longest relaxation time of the emulsion and corresponds to the relaxation of the shape of the droplets.

The interfacial tension is directly related to the secondary plateau in G'. It is the purpose of the following discussion to find the conditions for which this plateau actually exists and can be determined experimentally. This will lead us to discuss the influence of the emulsion parameters on the plateau modulus G_P and on the relaxation time λ_D. Clearly the secondary plateau will be defined if the relaxation times λ_D, λ_P, and λ_M are not too close:

$$\lambda_D \gg \lambda_P \gg \lambda_m$$

and

G_P > lowest measurable value on the instrument

(typically above 1–100 Pa, depending on

the type of instrument used) (11)

Estimation of Characteristic Relaxation Times and Moduli.

Figure 3 shows that parameters λ_D and G_P for the emulsion of viscoelastic liquids are very close to λ_1 and G_1 for the emulsion of Newtonian liquids in Figure 2. This can be understood by comparing the magnitudes of λ_1, which is of the order of $R\eta_m/\alpha$ (for K of the order of 1), to that of the relaxation time of the matrix $\lambda_m = \eta_m/G_m$. For blends of molten polymers, typical values are $R \sim 10^{-6}$ m and $\alpha \sim 10^{-3}$–10^{-2} N/m; if G_m is taken as the plateau modulus of the entanglement network ($G_m \sim 10^5$–10^6 Pa), it is found that usually $\lambda_1 \gg \lambda_m$. This means that if the secondary plateau exists, it occurs in a frequency range where $G^*_m \sim i\omega\eta_m$ and $G^*_i \sim i\omega\eta_i$. Thus the contribution to the storage modulus of the emulsion arising from the geometric relaxation of the droplets can be calculated as if the phases were Newtonian liquids of viscosities η_m and η_i. We take therefore to a first approximation:

$$\lambda_D \approx \lambda_1 = \frac{R\eta_m}{4\alpha}\frac{(19K + 16)(2K + 3 - 2\phi(K - 1))}{10(K + 1) - 2\phi(5K + 2)} \qquad (12)$$
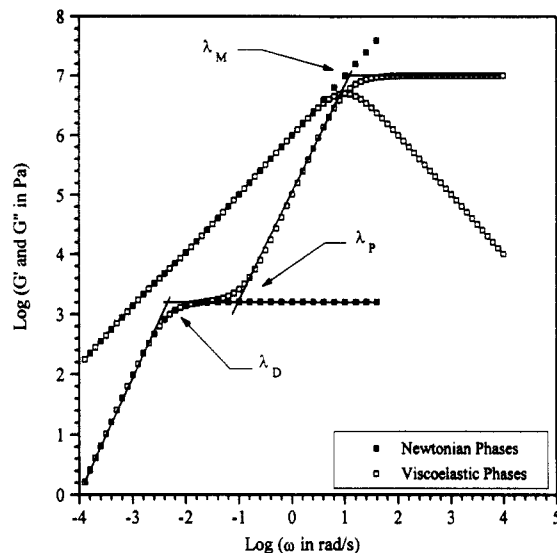

Figure 3. Dynamic moduli vs frequency; theoretical behavior for a blend of two viscoelastic liquids compared with a blend of two Newtonian liquids.

$$G_P \approx G_1 = 20\frac{\alpha}{R}\phi\frac{1}{(2K + 3 - 2\phi(K - 1))^2} \qquad (13)$$

Calculation of the high-frequency plateau modulus G_∞ is straightforward:

$$G_\infty = G_m\left\{\frac{4\alpha}{RG_m}(10(K + 1) + 3\phi(5K + 2)) + \right.$$

$$(19K + 16)(2K + 3 + 3\phi(K - 1))\right\}/\left\{\frac{4\alpha}{RG_m}(10(K + 1) - \right.$$

$$2\phi(5K + 2)) + (19K + 16)(2K + 3 - 2\phi(K - 1))\right\} \qquad (14)$$

which, if $\alpha/R \ll G_m$, amounts to

$$G_\infty \approx G_m\frac{2K + 3 + 3\phi(K - 1)}{2K + 3 - 2\phi(K - 1)} = G_m f(K,\phi) \qquad (15)$$

As indicated previously, this will most often be the case of polymer blends.

To estimate λ_M and λ_P, we assume that $\lambda_P \gg \lambda_M$ and compute the storage modulus of the emulsion in the frequency range $[1/\lambda_P, 1/\lambda_M]$. This amounts to neglecting interfacial tension (since droplet relaxation effects occur at lower frequencies) and taking the zero-frequency limit of eq 1. The following result is obtained for the storage modulus:

$$G' = \omega^2\eta_m\lambda_m\left[\frac{3(1 - \phi)(1 - \chi)}{2K + 3 - 2\phi(K - 1)} + \right.$$

$$\left.\frac{(2K + 3 + 3\phi(K - 1))(2K + 3\chi - 2\phi(K - \chi))}{(2K + 3 - 2\phi(K - 1))^2}\right]$$

$$G' = \omega^2\eta_m\lambda_m g(K,\chi,\phi) \qquad (16)$$

which is the terminal behavior of the matrix modified by some function g of K, χ, and ϕ. In the particular cases where inclusions and matrix have either the same relaxation time or the same viscosity, $g(K,\chi,\phi)$ takes the following simple expressions:

if $\chi = 1$

$$g(K,\chi,\phi) = \frac{2K + 3 + 3\phi(K-1)}{2K + 3 - 2\phi(K-1)} \qquad (17)$$

if $K = 1$

$$g(K,\chi,\phi) = 1 - \phi + \phi\chi \qquad (18)$$

The particular frequencies for which the quantity $\omega^2 \eta_m \lambda_m g(K,\chi,\phi)$ is respectively equal to G_P and G_∞ define the relaxation times λ_P and λ_M; thus

$$\lambda_M^2 = \frac{\eta_m \lambda_m}{G_\infty} g(K,\chi,\phi) = \lambda_m^2 \frac{g(K,\chi,\phi)}{f(K,\phi)} \qquad (19)$$

$$\lambda_P^2 = \frac{\eta_m \lambda_m}{G_P} g(K,\chi,\phi) \qquad (20)$$

Equations 12, 13, 15, 19, and 20 allow us to estimate the characteristic relaxation times and moduli of the emulsion from the viscoelastic parameters of the phases and to predict if a secondary plateau exists in the experimentally accessible frequency range.

Influence of Emulsion Parameters. From the above analysis, it is easy to discuss the influence of the viscoelastic parameters of the matrix and dispersed phase and of the emulsion parameters (α, R, ϕ) on the secondary plateau and characteristic relaxation times of the emulsion.

Viscosity Ratio. Figure 4 shows the influence of the viscosity ratio K ($K = 0.1, 1, 10, 100$), at constant matrix viscosity ($\eta_m = 10^6$ Pa·s) and constant relaxation times of the phases ($\lambda_m = \lambda_i = 0.1$ s). It is found that both λ_D and λ_P increase with increasing K, whereas the ratio λ_D/λ_P remains almost constant: This means that the width of the secondary plateau is not affected by the viscosity ratio. On the other hand, as is obvious from eq 13, the plateau modulus G_P scales as K^{-2} for values of K larger than unity and is almost constant for K lower than unity. This means that for highly viscous inclusions, experimental measurements in the secondary plateau zone are not easy since they involve low frequencies and low values of G'.

Relaxation Time of Matrix. On Figure 5, we show the influence of the relaxation time of the matrix at constant relaxation time of the inclusions ($\lambda_i = 0.1$ s, $\chi = 0.01, 0.1, 1$), all other parameters remaining constant. It appears that λ_P and λ_D become very close and the secondary plateau ill-defined when λ_m increases above a certain value ($\lambda_D/\lambda_P \sim 3$ for λ_m around 10 s and the parameters in Figure 5). The Cole–Cole diagrams ($\eta''(\omega)$ vs $\eta'(\omega)$) of the same data in Figure 6 clearly show the two relaxation mechanisms in the emulsion: the high-frequency relaxation of the phases and the low-frequency relaxation of the droplets, the two being well separated for low values of λ_m.

Interfacial Tension and Particle Radius. The influence of interfacial tension is represented in Figure 7. The plateau modulus G_P increases whereas the droplet relaxation time decreases with increasing α, as predicted by eqs 12 and 13. It also appears that the width of the secondary plateau decreases with increasing α. The opposite effects would be obtained for the influence of particle radius R since only the ratio α/R is involved in the constitutive equation.

Volume Fraction of Dispersed Phase. Figure 8 shows that increasing the volume fraction ϕ increases both G_P and the width of the secondary plateau by increasing slightly λ_D and decreasing λ_P.
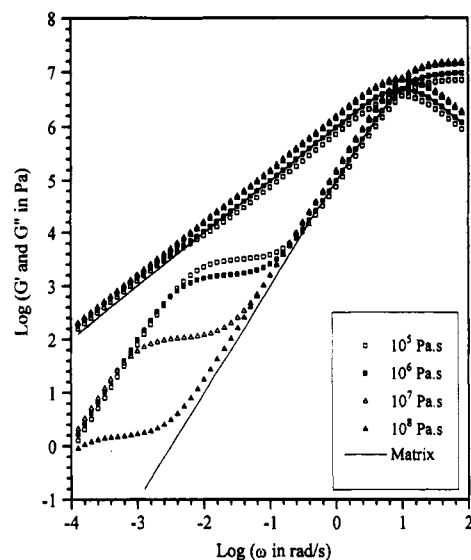

Figure 4. Dynamic moduli vs frequency; theoretical curves for blends of two viscoelastic liquids. Effect of the zero-shear viscosity of the dispersed phase.
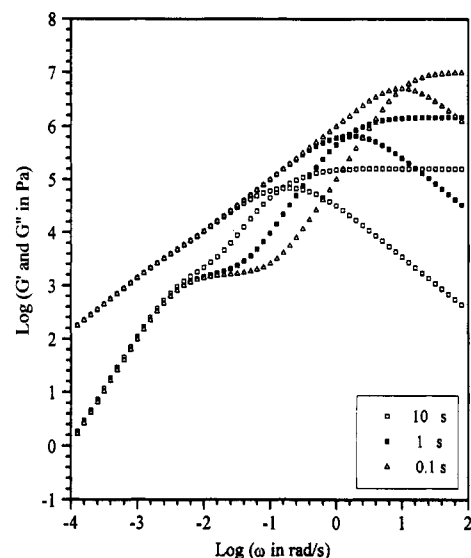

Figure 5. Dynamic moduli vs frequency; theoretical curves for blends of two viscoelastic liquids. Effect of the terminal relaxation time of the matrix.
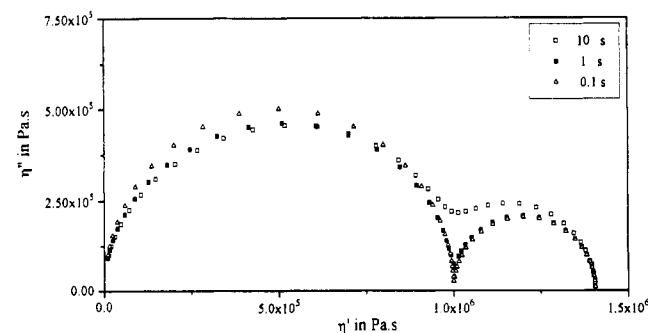

Figure 6. Cole–Cole diagrams; theoretical curves for blends of two viscoelastic liquids. Effect of the terminal relaxation time of the matrix.

Distribution of Particle Radius. Real blends are most often characterized by a nonuniform distribution of particle size. If the distribution is known, it may be taken into account for the calculation of the complex modulus of the emulsion, as shown by eq 1. However, it would make the model even more straightforward to use if the summation of the H_i terms over the distribution could be replaced by a single term involving some average radius.
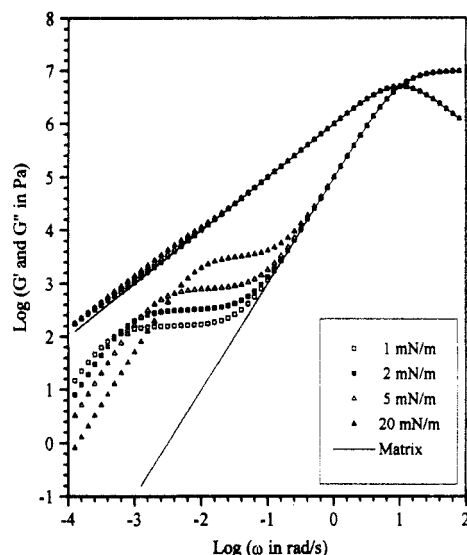
Figure 7. Dynamic moduli vs frequency; theoretical curves for blends of two viscoelastic liquids. Effect of the interfacial tension between the phases.
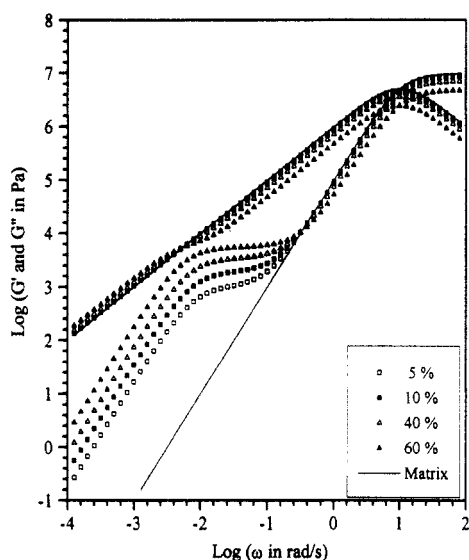

Figure 8. Dynamic moduli vs frequency; theoretical curves for blends of two viscoelastic liquids. Effect of the volume fraction in inclusions.

To determine what average should be taken, let us consider the zero-frequency limit of $H_i(\omega)$ for the case of Newtonian phases. The first-order expansion in ω is

$$H_i(\omega) = \frac{5K + 2}{10(K + 1)} - i\omega\frac{R_i\eta_m}{4\alpha}\left[\frac{19K + 16}{10(K + 1)}\right]^2 \quad (21)$$

It appears that in the terminal zone of an emulsion of Newtonian liquids

$$\sum\phi_iH_i(\omega,R_i) = \phi H(\omega,R_v) \quad (22)$$

where $\phi = \sum\phi_i$ is the total volume fraction of the dispersed phase and $R_v = (\sum\phi_iR_i)/\phi$ is the volume-average particle radius. To estimate the error made by using eq 22 over the whole frequency range, the sensitivity of the model predictions against polydispersity at constant R_v has been tested for various distributions represented in Figure 9 and the following values of the other parameters (corresponding roughly to one of the PDMS/POE-DO blends of section III.2): $\eta_m = 200$ Pa·s, $\eta_i = 150$ Pa·s, $\lambda_m = 0.02$ s, $\lambda_i = 0.001$ s, $\phi = 0.2$, and $\alpha = 10$ mN/m. Distributions I and IV are uniform; for I, II, and III, $R_v = 20$ μm whereas for IV, V, and VI, $R_v = 30$ μm. Table I lists the values of
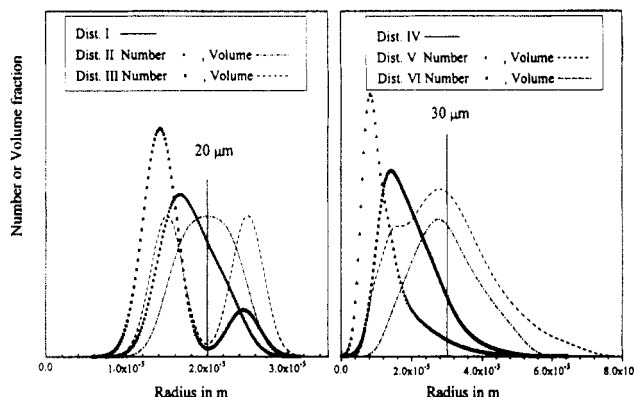

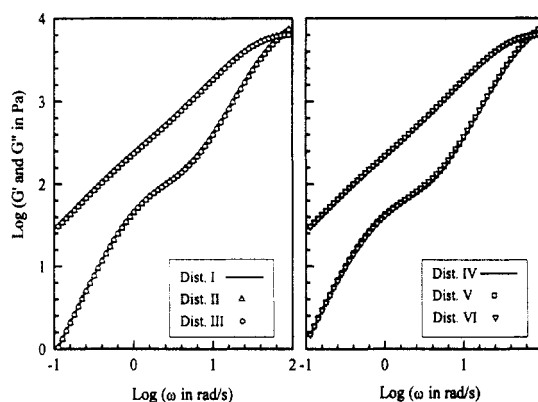**Figure 9.** Number of volume fraction of particles vs radius for five theoretical distributions.

Figure 10. Dynamic moduli vs frequency; theoretical curves for blends of two viscoelastic liquids. Effect of the polydispersity of particle size.

Table I

distribution	R_v (μm)	R_n (μm)	R_v/R_n
I	20	20.00	1.00
II	20	18.06	1.11
III	20	15.86	1.26
IV	30	30.00	1.00
V	30	19.79	1.52
VI	30	12.99	2.31

the number- and volume-average radii and of the polydispersity R_v/R_n. Distributions III and V are typical for those determined experimentally for the PDMS/POE-DO blends considered in section III.2. For some of these blends (containing POE-DO inclusions without interfacial agent; see section III.2), a bimodal distribution has been found with a polydispersity close to 1.2 and volume-average radius around 20 μm (distribution III). For the other blends (with interfacial agent) a somewhat broader distribution with higher R_v is found (distribution V).

Figures 10 and 11 clearly show that there is very little influence of particle size distribution at constant R_v on the model predictions in the secondary plateau up to values of polydispersity of the order of 2.3 (which is higher than for the blends considered in the present paper). As expected, polydispersity results qualitatively in a less well-defined secondary plateau as the consequence of a distribution of relaxation times. On the other hand, the behavior in the terminal zone only depends on R_v as predicted by the Newtonian analysis in eq 21.

As a consequence, eq 22 is a good approximation over the whole frequency range provided the polydispersity is not too high (typically lower than 2).

The next section will be devoted to a comparison of the model to experimental data. The main problem in applying the above discussion on characteristic relaxation
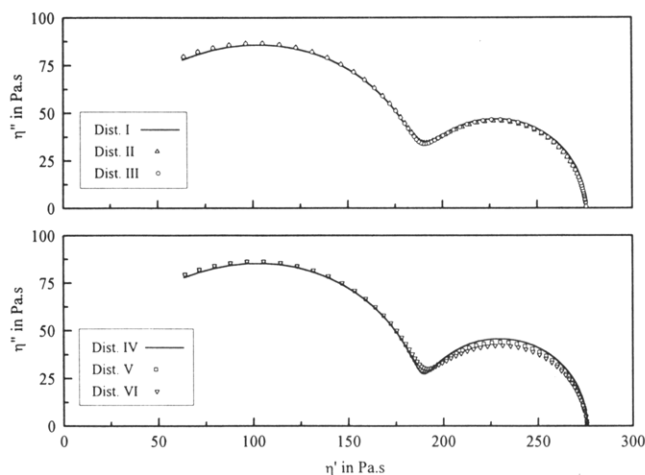
Figure 11. Cole–Cole diagrams; theoretical curves for blends of two viscoelastic liquids. Effect of the polydispersity of particle size.

Table II

	M_w	M_n	M_w/M_n
PS	92 000	88 000	1.07
PMMA	45 000	43 000	1.05

Table III

PS block			PS-*b*-PMMA			
M_w	M_n	M_w/M_n	% PS	M_w	M_n	M_w/M_n
26 000	24 000	1.06	52	50 000	47 000	1.06

times and moduli to the case of real blends arises from the distribution of particle sizes, which results in a less well-defined secondary plateau. Nevertheless, we will try to define these parameters by using an average particle radius. Moreover, eq 1 shows that if the distribution of particle radii is known, it may be taken into account for the calculation of the complex modulus of the emulsion.

III. Experimental Results

The present section is devoted to a comparison of the model to experimental data. According to the above discussion, we do not take into account the true distribution of particle size but use only the volume-average radius and apply eq 22.

1. PS/PMMA Blends. Products. PS and PMMA homopolymers and a PS–PMMA diblock copolymer were synthesized via anionic polymerization. The polystyrene sample was prepared by polymerization of styrene in benzene at 45 °C with butyllithium as the initiator. The PMMA homopolymer was obtained by polymerization in tetrahydrofuran at –70 °C using (diphenylmethyl)sodium as the initiator. The copolymer was prepared by first polymerizing the styrene in THF at –70 °C with (phenylisopropyl)potassium as the initiator. To avoid the attack of the ester group of MMA by the PS carbanion, 1,1-diphenylethylene was introduced prior to the addition of MMA to decrease the nucleophilicity of the active sites.[15] All polymerizations were conducted under high-purity argon in glass vessels equipped with Teflon valves.

Polymers were precipitated from solution by methanol and dried for several days in a vacuum oven at 40 °C. Polymer samples were characterized by means of size exclusion chromatography (GPC) coupled on line with viscosimetry, UV spectrometry, low-angle laser light scattering, and refractometry. The results are given in Tables II and III.

The Blends. Freeze-drying was used to prepare the blends: First, the homopolymers and the copolymer are
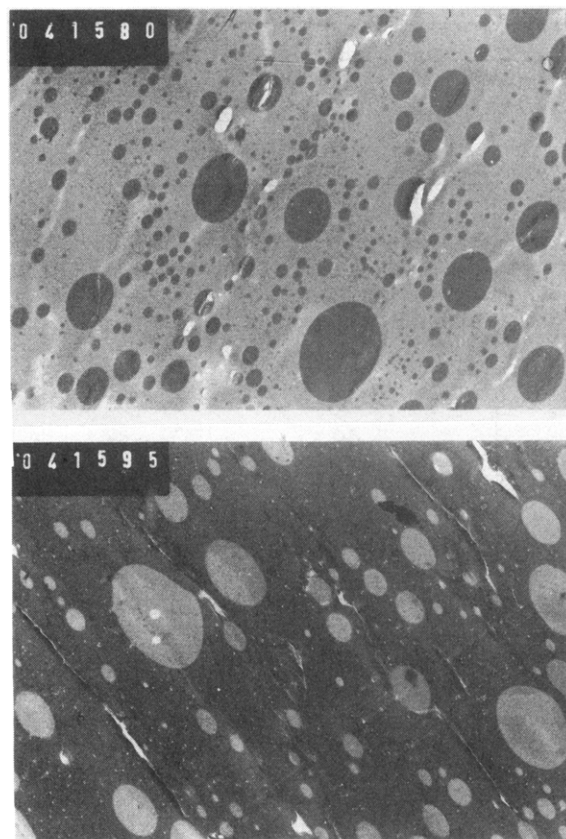

Figure 12. Morphology of the PS/PMMA blends by transmission electron microscopy. Reference 41580: blend MA PS/PMMA/COPO 78/19.5/2.5. Reference 41595: blend MB PS/PMMA/COPO 19.5/78/2.5.

solubilized separately in benzene at 5% in weight of polymer. After solubilization, given amounts of the three solutions are mixed to obtain the desired composition of the blend. The solution is agitated for 24 h. Finally, the solvent is removed by freeze-drying. Two blend compositions were prepared: MA, PS/PMMA/COPO 78/19.5/2.5 in weight; MB, PS/PMMA/COPO 19.5/78/2.5 weight.

Specimens for the rheological tests and morphological analysis were obtained by melting the obtained powder in a vacuum mold with a controlled thermal history: After 30 min at 70 °C, the temperature is increased at a rate of 300 °C/h to 180 °C and maintained at this value for 30 min. Return to room temperature takes about an hour.

Figure 12 gives an idea of the morphology of the blends after the rheological measurements as observed by TEM on a Philips EM 30 microscope. Cuts of thickness between 60 and 90 nm were prepared by microtoming at room temperature; this induces a slight elongation of the sample in the direction of the cut. Selective degradation of PMMA under the electron beam gives the observed contrast.

A rather broad size distribution is obtained, with radii of inclusions between 1.5 and 0.05 µm. The precise determination of the volume-average radius was more readily performed on the PDMS/POE-DO blends in section III.2, and the discussion of model predictions for the PS/PMMA blends will remain on a qualitative level. However, Figure 12 shows that the morphology is very close for MA and MB, which will allow us to illustrate the influence of the viscosity ratio.

Rheological Measurements. The dynamic measurements were carried out on a Rheometrics RMS 605 mechanical spectrometer using a parallel-plate geometry (radii of the specimens: 12.5 and 25 mm for each phase and 12.5 mm for the blends). The experiments were carried

Table IV[a]

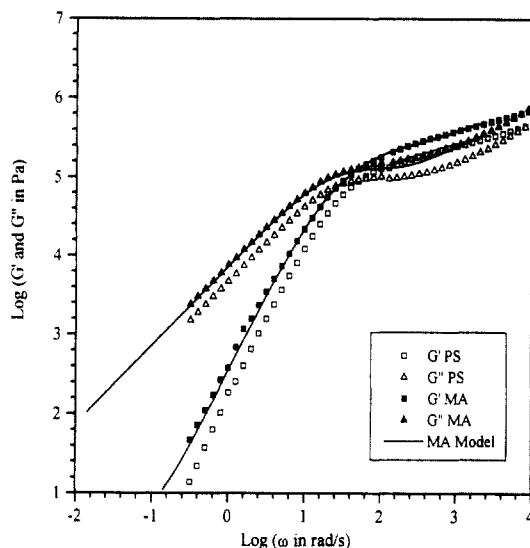|	PS	PMMA
η_0 (Pa·s)	4760	220 000
λ (s)	0.03	0.63

[a] At 180 °C.

Figure 13. Dynamic moduli vs frequency. Blend MA PS/PMMA/COPO 78/19.5/2.5 at 180 °C.
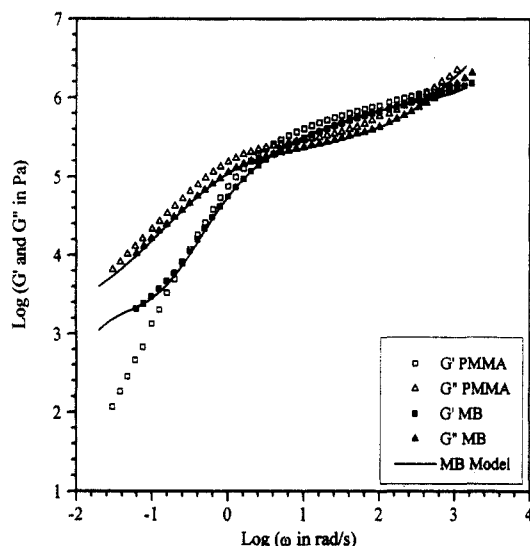

Figure 14. Dynamic moduli vs frequency. Blend MB PS/PMMA/COPO 19.5/78/2.5 at 180 °C.

out in the temperature range 140–200 °C, and data at different temperatures were reduced to 180 °C using time–temperature superposition. The temperature is measured with a precision of ±0.1 °C within the metallic plate in contact with the polymer melt. Depending on the temperature and frequency, the strain amplitude was taken between 2.5 and 20% to obtain a high enough value of the torque. It was always verified that the behavior of the sample was in the range of linear viscoelasticity.

Results and Discussion. The zero-shear viscosities and the terminal relaxation times of the phases (PS and PMMA) at 180 °C are given in Table IV: the ratio η_i/η_m of the zero-shear viscosities is 46 for MA and 0.022 for MB. Figures 13–16 compare the rheological behavior of the blends to that of the matrix polymer, i.e., blend MA and PS on Figures 13 and 15, and blend MB and PMMA on Figures 14 and 16.

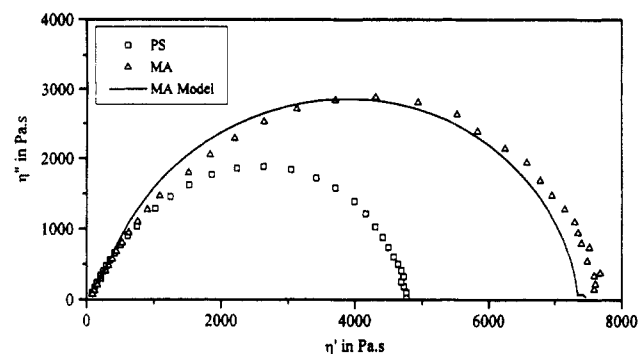The data show that the secondary plateau in G' only appears for blend MB. By assuming that eq 22 holds, eq

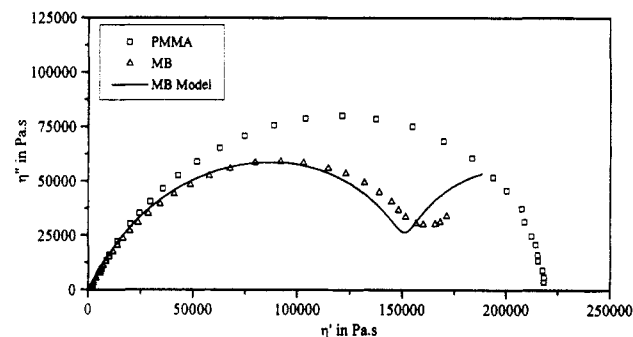**Figure 15.** Cole–Cole diagrams. Blend MA PS/PMMA/COPO 78/19.5/2.5 at 180 °C.

Figure 16. Cole–Cole diagrams. Blend MB PS/PMMA/COPO 19.5/78/2.5 at 180 °C.

Table V[a]

	MA PS/PMMA/COPO 78/19.5/2.5	MB PS/PMMA/COPO 19.5/78/2.5
η_0 (Pa·s)	7600	270 000
λ_D (s)	37	56
λ_P (s)	9	7
λ_M (s)	0.04	0.6
G_P (Pa)	4	2000

[a] At 180 °C.

1 allows us to estimate the ratio α/R_v as the value leading to the best agreement between experimental and theoretical curves in the low-frequency range (the other parameters, volume fraction and the dynamic moduli of the phases, are experimental quantities). The value of α/R_v used for the calculated curves in Figures 14 and 16 is 5880 Pa.

If the same value of α/R_v is used to describe the behavior of the blend MA, the calculated curves in Figures 13 and 15 are obtained. The model clearly accounts for the fact that no secondary plateau exists for this blend in the experimentally accessible range of frequency and modulus.

The characteristic relaxation times and secondary plateau moduli were estimated for both blends by assuming that the phases can be described by single relaxation time Maxwell models with parameters of Table IV and by taking α/R_v = 5880 Pa. The values are given in Table V. Relaxation times λ_D and λ_P are of the same order of magnitude for both blends, indicating that the secondary plateau for MA and MB occurs in the same frequency range. On the other hand, the value of the secondary plateau modulus G_P is about three decades lower for blend MA than for blend MB. With the transducer and geometry used, this value (4 Pa) is out of the experimentally accessible range.

The estimation of interfacial tension from these viscoelastic data would require a precise knowledge of the volume-average particle radius. As already indicated, this

Table VI[a]

| | POE-DO 35 000 | PDMS | | |
		47V30 000	47V125 000	47V500 000
η_0 in Pa·s	169	13.5	91	212
λ in s	0.001	0.002	0.01	0.02

[a] At 70 °C.

will be much easier for PDMS/POE-DO blends (for which an original method of morphological analysis has been proposed) than for the PS/PMMA blends. Nevertheless, a range of values for interfacial tension can be estimated from the ratio $\alpha/R \sim 6000$ Pa and the distribution of particle radii (0.05–1.5 μm). The obtained range for α (0.3–9 mN/m) covers the right order of magnitude (for PS/PMMA without copolymer at 180 °C, $\alpha = 1.12$ mN/m[16]). The main interest of the blends MA and MB is that they have very close morphologies and contain the same amount of copolymer, the only difference being that they have inverted matrix and dispersed phase. The obtained agreement between experimental data and the emulsion model for both blends supports the idea that the long-time relaxation mechanisms are due to geometrical relaxation of suspended droplets.

To achieve a more quantitative comparison between model and experimental data, another series of measurements have been carried out on PDMS/POE-DO blends.[17,18]

2. PDMS/POE-DO Blends. Products. The POE-DO sample was a commercial polymer (Hoechst PEG 35000) with a melting point of 62 °C and a weight-average molecular weight of 35 000. The three PDMS samples were also commercial products (Rhône Poulenc Rhodorsil 47V30 000, 47V125 000, and 47V500 000). The zero-shear viscosities and relaxation times of all phases at 70 °C are given in Table VI. For the second series of blends, we used an interfacial agent with the following chemical structure (Lutensol AP9 from BASF): $H_{19}C_9(C_6H_4)O(CH_2CH_2O)_9H$.

The Blends. With this pair of polymers, we can separate the fabrication of the POE-DO inclusions from the blending itself.

First Step (Fabrication of the Inclusions). Inclusions with interfacial agent: In a double-walled reactor, comprising a system of agitation, we placed 680 g of a low-viscosity PDMS (Rhodorsil 47V2000, $\eta_0 \sim 2$ Pa·s at 20 °C), 68 of POE-DO 35 000, and 6.8 g of interfacial agent. The mixture was kept for 1 h at 70 °C and then refrozen under agitation.

Inclusions without interfacial agent: In this case, we placed in the reactor 980 g of a silicone oil (Rhodorsil, $\eta_0 \sim 20$ Pa·s at 20 °C) and 20 g of POE-DO 35 000. The blend was kept under agitation for 1 h at 80 °C and then refrozen quickly without agitation.

For the two processes, the oil was removed by washing with *n*-hexane. The particles thus obtained were dried at 40 °C and then kept at 20 °C at reduced pressure to prevent the absorption of water.

Second Step (Blending). After a crude mixing, following removal of gas, the blends were homogenized with the help of continuous shearing at ambient temperature in the rheometer. POE-DO is a solid at room temperature ($T < T_m$) and the continuous shearing does not modify the size and the polydispersity in size of the inclusions. The temperature is then increased to the temperature of measurement (70 °C) without any further steady shear flow. It can be expected that the dynamic measurements do not alter the distribution in size of the particles. This was verified by characterizing the particle
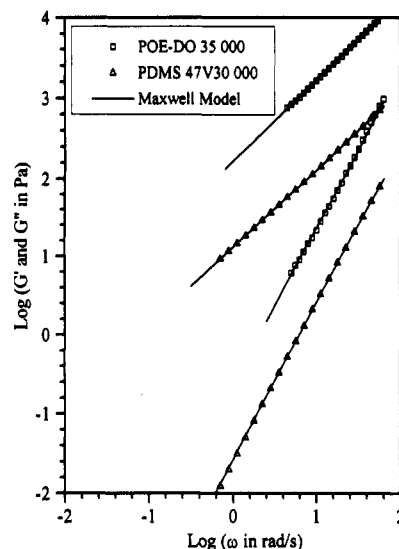

Figure 17. Dynamic moduli vs frequency. POE-DO 35 000 and PDMS 47V30 000 at 70 °C.
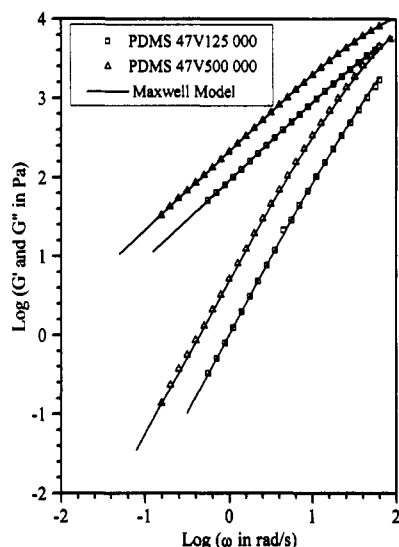

Figure 18. Dynamic moduli vs frequency. PDMS 47V125 000 and PDMS 47V500 000 at 70 °C.

size distribution in the blends after the rheological measurements. The blends were realized with the following values of volume fraction of POE-DO inclusions: 5, 10, 15, and 20% (for the blends with interfacial agent); 7.5 and 15% (for the blends without interfacial agent).

Morphology. It is possible to characterize the morphology at room temperature of the dispersed phase by direct observation of the inclusions before blending. The size and the polydispersity in size of inclusions were studied by optical microscopy. For the inclusions without interfacial agent, a bimodal type distribution is found; the number- and volume-average radii determined from several photographs are respectively about 15 and 20 μm. For the inclusions with interfacial agent, a monomodal but somewhat broader distribution is obtained with a volume-average radius of about 40 μm. The rheological behavior is calculated from eqs 1 and 22 by using the above values of R_v.

Rheological Measurements. The dynamic viscoelastic measurements were carried out on a controlled-stress rheometer (Carrimed CSL 100) with a cone-and-plate geometry (cone angle 4°, radius 30 mm). The maximal torque on this apparatus is 10^{-2} N m, and the frequency range is from 10 to 10^{-3} Hz (63–0.0063 rad/s). The temperature of the fluid during the experiment is 70 ± 0.1
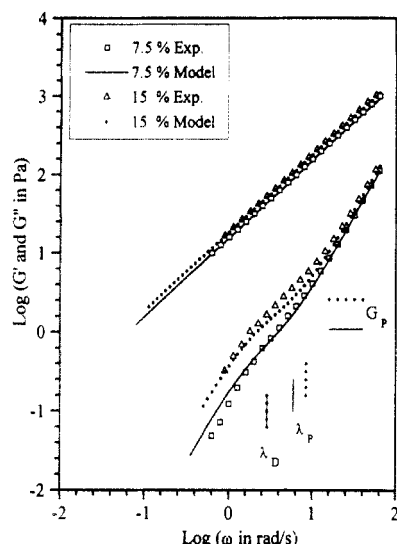
Figure 19. Dynamic moduli vs frequency. Blends PDMS 47V30 000 + POE-DO 35 000 without interfacial agent at 70 °C.
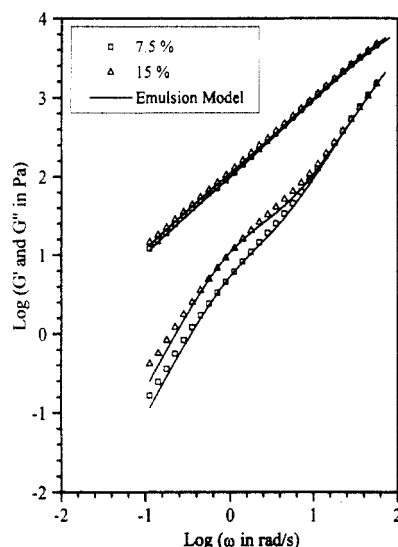

Figure 20. Dynamic moduli vs frequency. Blends PDMS 47V125 000 + POE-DO 35 000 without interfacial agent at 70 °C.

Figure 21. Dynamic moduli vs frequency. Blends PDMS 47V500 000 + POE-DO 35 000 without interfacial agent at 70 °C.

Figure 22. Cole–Cole diagrams. Blends PDMS 47V500 000 + POE-DO 35 000 without interfacial agent and matrix at 70 °C.

Figure 23. Dynamic moduli vs frequency. Blends PDMS 47V125 000 + POE-DO 35 000 with interfacial agent at 70 °C.

°C. Depending on the frequency, the strain amplitude was taken between 1 and 6% to obtain a high enough value of torque. For all measurements, it was verified that the behavior of the sample was linear viscoelastic.

Rheological Results and Discussion. The rheological data for the different blends are shown respectively in Figures 19–22 for the blends without interfacial agent, and Figures 23 and 24 for the blends with interfacial agent.

In the first case (without interfacial agent), all parameters of the emulsion model are known: The dynamic moduli of the phases are experimental data (Figures 17 and 18) and we take $R_v = 20 \mu m$. The experimental value of $\alpha_{PDMS/POE-DO}$ obtained from direct measurements[19] is 10.8 mN/m at 20 °C and 10.2 mN/m at 100 °C, and $-(\delta\alpha/\delta T) = 0.0078$ mN/m °C^{-1}; at 70 °C the value would be 10.4 mN/m.

Figures 19–21 show that a good agreement between theoretical and experimental curves is obtained over the whole frequency range for different values of the ratio of zero-shear viscosities (between 0.8 and 13) and volume fraction of dispersed phase. The Cole–Cole diagrams (Figure 22) provide another way to represent these data and confirm the excellent overall agreement with the emulsion model.
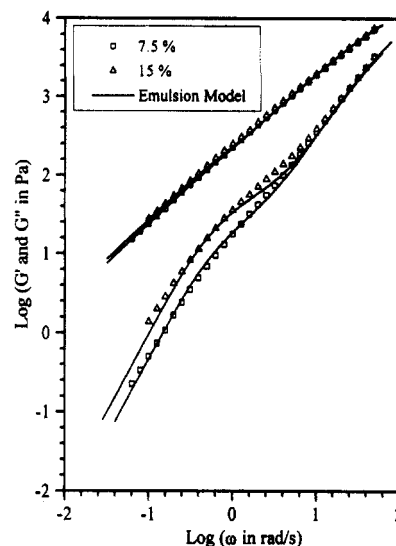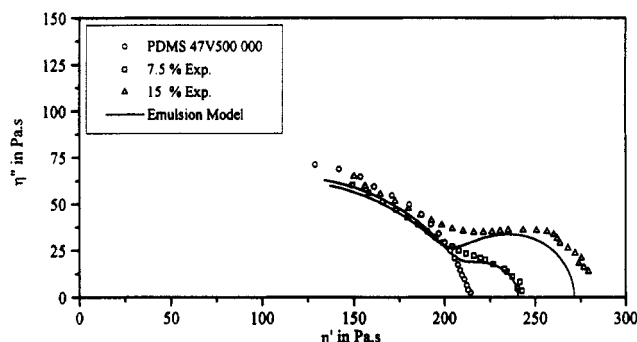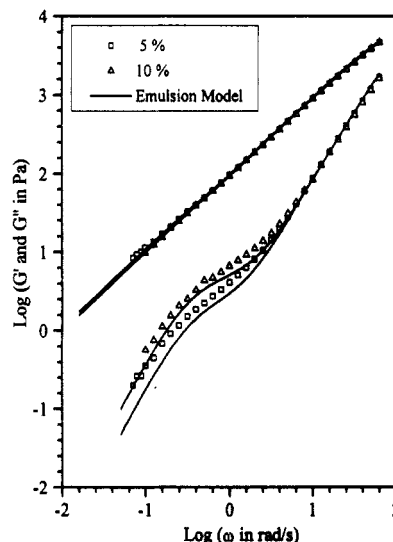
The characteristic parameters λ_D, λ_P, λ_M, and G_P of the six blends without compatibilizer were estimated by using eq 12, 13, 19, and 20. The zero-shear viscosities and relaxation times of the phases that appear in these expressions were determined from the rheological data in Figures 17 and 18 and are listed in Table VI. The particle size was taken as the volume-average radius.

Table VII shows that for all blends λ_M is much smaller (at least one decade) than λ_D and λ_P, the characteristic relaxation times of the secondary plateau. Although the ratio between λ_D and λ_P is lower (of the order of 3 for all
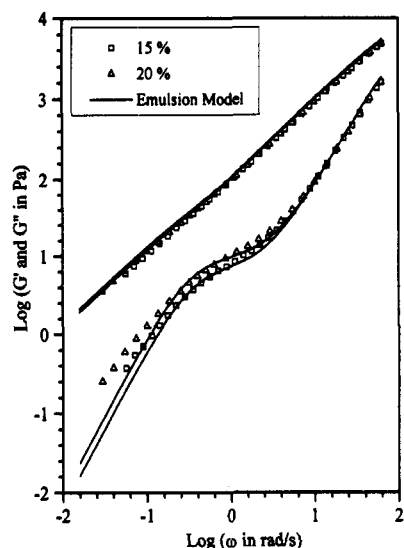
Figure 24. Dynamic moduli vs frequency. Blends PDMS 47V125 000 + POE-DO 35 000 with interfacial agent at 70 °C.

Table VII

	PDMS					
	47V30 000		47V125 000		47V500 000	
ϕ (%)	7.5	15	7.5	15	7.5	15
η_0 (Pa·s)	16	19	105	122	240	271
λ_D (s)	0.35	0.35	0.60	0.60	0.86	0.91
λ_P (s)	0.17	0.12	0.22	0.15	0.32	0.22
λ_M (s)	0.002	0.002	0.009	0.008	0.017	0.016
G_P (Pa)	1.1	2.6	18	37	36	71

blends), the data in Figures 19–21 show that the secondary plateau is well defined. Figure 19 shows that the calculated values of λ_D, λ_P, and G_P are in good accordance with the experimental $G'(\omega)$ curves. The existence and the position of this plateau may therefore be predicted by the values of these three parameters.

For the blends with interfacial agent, the only unknown parameter is the interfacial tension between the phases. By taking always the volume-average radius in the theoretical expression of $G^*(\omega)$, the value of interfacial tension leading to the best agreement between calculated and experimental curves is close to 4 mN/m (Figures 23 and 24). Because of the addition of an interfacial agent, the expected value of α should indeed be smaller than 10.4 mN/m.

IV. Conclusion

The experimental data obtained for the PS/PMMA and PDMS/POE-DO blends confirm that the emulsion model discussed in the present paper is able to describe quan-titatively the linear viscoelastic properties of two-phase polymer blends in the melt.

In the case of the PS/PMMA blends, we have shown the major effect of the viscosity ratio of the phases on the storage modulus in the low-frequency range. This result supports the assumption that the long-time relaxation mechanisms are due to geometrical relaxation of the droplets of the dispersed phase.

The secondary plateau for $G'(\omega)$ can be characterized by three parameters (two relaxation times, λ_D and λ_P, and a modulus (G_P) which may be estimated from the viscoelastic properties of the phases, the volume fraction and volume-average particle size of the dispersed phase, and the interfacial tension. From the values of these parameters one can predict if the secondary plateau is accessible experimentally, depending on the frequency range and minimum torque value available on the rheometer.

In this case, an estimation of the interfacial tension from viscoelastic data is possible, provided the volume-average radius of the dispersed particles is known and the polydispersity $\bar{R}_v/\bar{R}_n$ does not exceed a value of about 2. The results for the PDMS/POE-DO blends, for which the morphology could be precisely determined, show that dynamic shear measurements can be used as a new and original method to determine the interfacial tension between two polymer melts.

References and Notes

 (1) Einstein, A. *Ann. Phys.* **1906**, *No. 19*, 289.
 (2) Einstein, A. *Ann. Phys.* **1911**, *No. 34*, 591.
 (3) Taylor, G. I. *Proc. R. Soc. London* **1932**, *A132*, 41.
 (4) Taylor, G. I. *Proc. R. Soc. London* **1934**, *A146*, 501.
 (5) Frolich, H.; Sack, R. *Proc. R. Soc. London* **1946**, *A185*, 415.
 (6) Oldroyd, J. G. *Proc. R. Soc. London* **1953**, *A218*, 122.
 (7) Oldroyd, J. G. *Proc. R. Soc. London* **1955**, *A232*, 567.
 (8) Kerner, E. H. *Proc. Phys. Soc.* **1956**, *69*, 808.
 (9) Uemura, S.; Takayanagi, M. *J. Appl. Polym. Sci.* **1966**, *10*, 113.
(10) Schowalter, W. R.; Chaffey, C. E.; Brenner, H. *J. Colloid Interface Sci.* **1968**, *26*, 152.
(11) Dickie, R. A. *J. Appl. Polym. Sci.* **1973**, *17*, 45.
(12) Choi, S. J.; Schowalter, W. R. *Phys. Fluids* **1975**, *18*(4), 420.
(13) Palierne, J.-F. *Rheol. Acta* **1990**, *29*, 204.
(14) Han, C. D.; Huang, H. K. C. *J. Appl. Polym. Sci.* **1985**, *30*, 4431.
(15) Freyss, D.; Leng, M.; Rempp, P. *Bull. Soc. Chim. Fr.* **1964**, 221.
(16) Wu, S. *J. Phys. Chem.* **1970**, *74*(3), 32.
(17) Graebling, D.; Muller, R. *J. Rheol.* **1990**, *34*, 193.
(18) Graebling, D.; Muller, R. *Colloids Surf.* **1991**, *55*, 89.
(19) Roe, R. J. *J. Colloid Interface Sci.* **1969**, *31*, 228.